JCB Article

Brain development in mice lacking L1–L1 homophilic adhesion

Kyoko Itoh,[1,2] Ling Cheng,[1] Yoshimasa Kamei,[1] Shinji Fushiki,[2] Hiroyuki Kamiguchi,[3] Paul Gutwein,[4] Alexander Stoeck,[4] Bernd Arnold,[5] Peter Altevogt,[4] and Vance Lemmon[1,6]

[1]Department of Neuroscience, Case Western Reserve University, Cleveland, OH 44106
[2]Department of Pathology and Applied Neurobiology, Kyoto Prefectural University of Medicine, Kyoto 602-0841, Japan
[3]Developmental Brain Science Group, RIKEN Brain Science Institute, Saitama 351-0198, Japan
[4]D010 and [5]D050 Tumor Immunology Program, German Cancer Research Center, D-69120 Heidelberg, Germany
[6]The Miami Project to Cure Paralysis, University of Miami School of Medicine, Miami, FL 33136

A new mouse line has been produced in which the sixth Ig domain of the L1 cell adhesion molecule has been deleted. Despite the rather large deletion, L1 expression is preserved at normal levels. In vitro experiments showed that L1–L1 homophilic binding was lost, along with L1-α5β1 integrin binding. However, L1–neurocan and L1–neuropilin binding were preserved and sema3a responses were intact. Surprisingly, many of the axon guidance defects present in the L1 knockout mice, such as abnormal corticospinal tract and corpus callosum, were not observed. Nonetheless, when backcrossed on the C57BL/6 strain, a severe hydrocephalus was observed and after several generations, became an embryonic lethal. These results imply that L1 binding to L1, TAG-1, or F3, and L1-α5β1 integrin binding are not essential for normal development of a variety of axon pathways, and suggest that L1–L1 homophilic binding is important in the production of X-linked hydrocephalus.

Introduction

L1 is one of the most intensely studied adhesion molecules expressed in the developing central and peripheral nervous system (Kamiguchi et al., 1998). L1 is important in neuronal migration, axon growth, guidance, fasciculation, and synaptic plasticity. L1 is also expressed in nonneuronal cells such as the immune system, kidney, pigment cells, and a variety of cancers. L1 is a member of the Ig superfamily and binds to several extracellular ligands, such as the proteoglycan neurocan, integrins, axonin-1/TAG-1, and contactin/F3/F11, as well as binding to itself in a homophilic manner. L1 is an integral membrane protein with six Ig domains, five fibronectin (FN) type III domains, and a highly conserved cytoplasmic tail. It has been reported that all immunoglobulin domains Ig1–Ig6 and the FN 2 domain of L1 are involved in homophilic binding (Zhao and Siu, 1995; Zhao et al., 1998; De Angelis et al., 1999, 2001; Kenwrick et al., 2000; Jacob et al., 2002). The first Ig domain supports binding to neurocan (Oleszewski et al., 2000). The sixth Ig domain, which contains RGD sequences (two in mice, one in humans), is capable of promoting neurite growth for some (but not all) neurons by binding to an integrin or homophilically to L1 itself (Ruppert et al., 1995; Montgomery et al., 1996; Yip et al., 1998; Weller and Gartner, 2001). The third FN domain also has an integrin-binding site (Silletti et al., 2000). Finally, L1 also functions in repellent cell interactions with the first Ig domain binding to neuropilin to form a coreceptor for sema3a (Castellani et al., 2000, 2002).

A number of X-linked forms of mental retardation have been linked to mutations in the L1 gene, including X-linked hydrocephalus, MASA syndrome (mental retardation, aphasia, shuffling gait, adducted thumbs), agenesis/dysgenesis of the corpus callosum, and X-linked spastic paraplegia (Kamiguchi et al., 1998). Symptoms vary among affected family members and between families, and 143 different mutations in the human L1 gene have been reported (Weller and Gartner, 2001). More severe consequences are associated with mutations of the extracellular region, which may disrupt adhesion and signaling, whereas milder symptoms occur with mutations in the cytoplasmic domain, which may alter only signaling or interactions with the cytoskeleton (Yamasaki et al., 1997; Kamiguchi et al., 1998).

Address correspondence to Vance Lemmon, The Miami Project to Cure Paralysis, University of Miami School of Medicine, Lois Pope LIFE Center, Room 4-16, 1095 NW 14th Terrace, Miami, FL 33136. Tel.: (305) 243-6793. Fax: (305) 243-3160. email: vlemmon@miami.edu

Key words: adhesion; hydrocephalus; L1cam; corticospinal tract; integrin

Abbreviations used in this paper: CNS, central nervous system; DRG, dorsal root ganglion; FN, fibronectin; KO, knockout; wt, wild-type.

The Journal of Cell Biology, Volume 165, Number 1, April 12, 2004 145–154
http://www.jcb.org/cgi/doi/10.1083/jcb.200312107

The Journal of Cell Biology

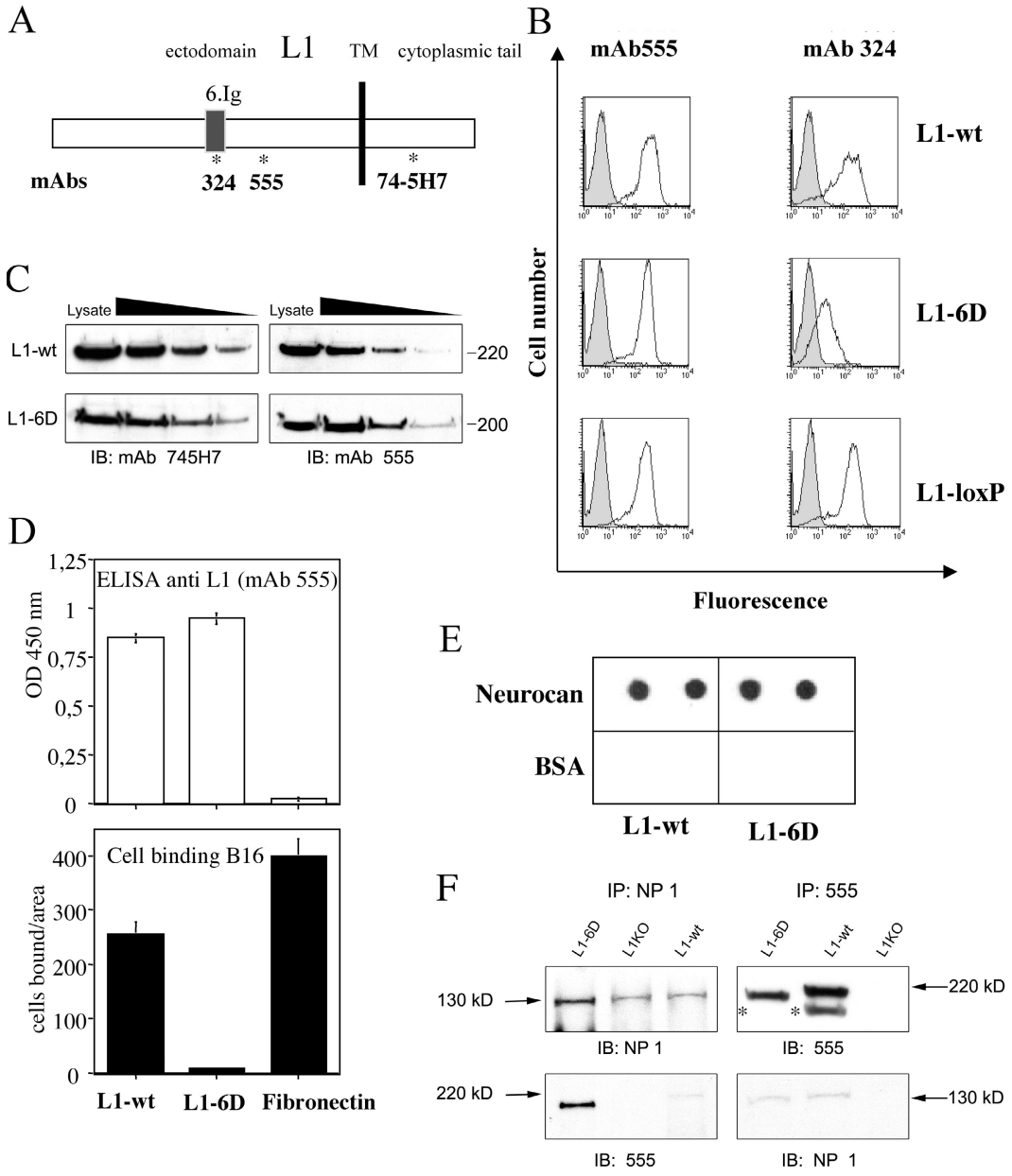

Figure 1. **Analysis of L1-6D expression.** (A) Map of L1 indicating location of mAb-binding sites by asterisks: 555 binding within the FN repeats, 324 at the sixth Ig domain, and 74-5H7 in the cytoplasmic domain of L1. (B) FACS® analysis of L1 expression on splenic lymphocytes from wt mice (L1-wt), mice with the L1 sixth Ig domain deleted (L1-6D), and exons coding for the sixth Ig domain surrounded by loxP sites and containing a neomycin cassette (L1-loxP). mAb 555 shows equal expression levels on all three types of splenic lymphocytes, but mAb 324 shows reduced expression in L1-6D mice. (C) Western blot analysis of L1 expression from lymphocytes from L1-wt and L1-6D mice. Two different antibodies showed similar expression levels in both types of mice. (D) Attachment of B16F10 cells to L1 purified from L1-wt and L1-6D or FN. ELISA showed that similar amounts of L1 were coated onto the glass substrates, but the B16F10 cells bound to L1-wt (but not L1) from the L1-6D mice. The cells also bound to FN. (E) L1 binding to neurocan. Neurocan was immobilized on Immobilon membranes and was incubated with purified L1 from L1-wt and L1-6D mice. Bound L1 was detected by mAb 555. Both types of L1 were able to bind to neurocan, but not to BSA. (F) L1 binding to neuropilin. Neuropilin-1 (NP 1) was immunoprecipitated, and the immunoprecipitation was probed on Western blots with antibodies to NP1 and L1. L1 was found in the immunoprecipitations from wt and L1-6D mice, but not L1-KO mice. The reverse immunoprecipitation, with anti-L1 (antibody 555), revealed NP1 in the immunoprecipitations from L1-6D mice and wt mice, but no NP1 immunoreactivity was seen in L1 immunoprecipitation from L1-KO mice. Asterisk indicates the L1 cleavage fragment L1-180.

Knockouts of the L1 gene in mice (L1-KO mice) have been generated in two laboratories, and have been intensely examined in order to define the molecular basis of human syndromes with L1 (Dahme et al., 1997; Cohen et al., 1998; Fransen et al., 1998). L1-KO mice showed reduced corticospinal tract, abnormal pyramidal decussation, decreased axonal association with nonmyelinating Schwann cells, ventricular dilatation, and hypoplasia of the cerebellar vermis. Demyanenko and colleagues reported abnormal morphogenesis of cortical dendrites, showing that pyramidal neurons in layer V exhibited undulating apical dendrites that did not reach layer I, as well as a smaller hippocampus with

fewer pyramidal and granule cells (Demyanenko et al., 1999) and altered distribution of dopaminergic neurons in the brain of L1 null mice (Demyanenko et al., 2001). There is also a reduced size of corpus callosum because of the failure of many callosal axons to cross the midline. These findings suggest a variety of biological roles for L1 that are critical in brain development in different brain regions.

To assess which of the L1 interactions underlie the defects observed in the L1-KO mice, we generated a new knock-in mouse in which the sixth Ig domain of L1 was deleted (L1-6D). This deletion would be expected to prevent L1–L1 homophilic binding and L1 binding to RGD-dependent integrins, but not to disrupt interactions with neurocan or neuropilin. As expected, cerebellar granule cells from L1-6D mice on the 129/Sv background exhibited neither adhesion nor axonal growth on an L1-Fc substrate, whereas L1 binding to neurocan and neuropilin was preserved. The L1-6D/129/Sv mice brains showed normal development of the decussation of the corticospinal tract, thalamocortical tract, and corpus callosum, as well as appropriate anatomical features. The results show that axonal guidance and neuronal migration in the central nervous system (CNS) of 129/Sv mice can develop normally without L1 binding to L1, TAG-1, F3, and β1 integrin, in marked contrast to the L1-KO mice. Interestingly, like the L1-KO mice (Dahme et al., 1997), crossing the L1-6D mutation onto the C57BL/6 background resulted in a dramatic hydrocephalus. By the fifth backcross to C57BL/6, the L1-6D mutation caused embryonic lethality. These results suggest that L1 homophilic binding underlies the L1-induced hydrocephalus and lethality on some genetic backgrounds.

Results

L1-6D does not support α5β1 integrin binding or L1 homophilic binding, but does bind neurocan and neuropilin

mAbs to different regions of mouse L1 were used for the initial characterization of L1-6D mice (see binding sites of mAbs in Fig. 1 A). Splenic lymphocytes from 129/Sv mice, L1-6D mice, or animals in which the L1 sixth Ig domain was targeted by loxP but not deleted were tested by fluorescent staining with the two mAbs against the ectodomain of L1, mAbs 324 and 555, respectively. As shown in Fig. 1 B, mAb 555 staining was similar on all cell populations analyzed. In contrast, mAb 324, which recognizes an epitope close to the sixth Ig domain and can block RGD-dependent binding to L1 (Ruppert et al., 1995), showed reduced staining on L1-6D splenocytes. These findings show that L1 in L1-6D mice was expressed at comparable levels to control mice, but was structurally altered. To verify that the L1 cytoplasmic part was correctly expressed after Cre-mediated deletion of the sixth domain, wild-type L1 (L1-wt) and L1-6D splenic lysates were probed by Western blot analysis with mAb 74-5H7, an antibody that binds to the L1 cytoplasmic domain (Schaefer et al., 2002). As shown in Fig. 1 C, the mAb recognized L1-wt and L1-6D at similar levels. Most noteworthy, L1-6D was ~20 kD smaller in size than L1-wt.

The sixth domain of L1 supports integrin-mediated binding of cells to L1 (Ruppert et al., 1995; Oleszewski et al., 2000). Previous work has shown that B16F10 melanoma cells bind to L1 via α5β1, and cell binding is totally abolished by mAbs to α5 and β1 integrins or by mutagenesis of both RGD sequences in the sixth domain (Oleszewski et al., 2000). To investigate whether L1 from L1-6D mice showed impaired integrin-mediated binding, L1-6D and L1-wt, for control, were isolated by immunoaffinity purification from spleen and brain Triton X-100 lysates. Eluted peak fractions of each affinity column were coated to glass slides and tested for B16F10 cell binding. As shown in Fig. 1 D, purified L1-6D was unable to support B16F10 cell binding due to the lack of RGD sites in the deleted sixth domain. Binding of cells to L1-wt and FN was as expected from previous work (Oleszewski et al., 2000).

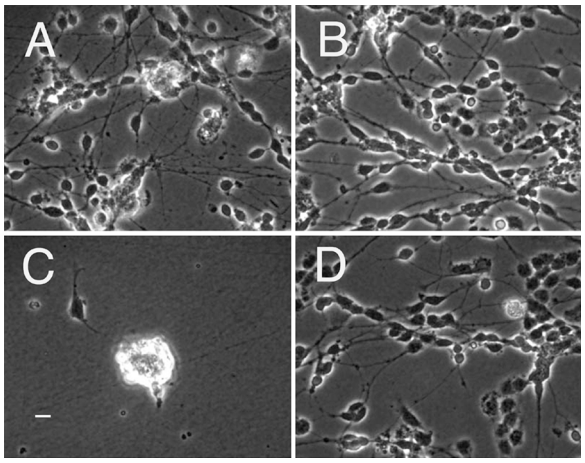

Figure 2. **Cerebellar neurons from L1-6D mice fail to attach to L1.** Neurons from L1-wt (A and B) and L1-6D (C and D) were incubated in dishes coated with purified L1 (A and C) or laminin (B and D). Although L1-wt neurons attach and send out neurites on both L1 and laminin, the L1-6D neurons do not attach or send out neurites on L1. Bar, 5 μm.

To further prove that L1-6D was functionally active, we analyzed its binding to neurocan. Neurocan interacts with L1 via the first Ig domain (Oleszewski et al., 2000). As shown in Fig. 1 E, both L1-wt and L1-6D could efficiently bind to immobilized neurocan. Collectively, the results suggest that L1-6D has lost the ability to support α5β1 integrin binding, but is still capable of interacting with neurocan.

L1 has been shown to interact with neuropilin via the first Ig (Castellani et al., 2002) and to participate in sema3a signaling (Castellani et al., 2000). Immunoprecipitations of neuropilin-1 from L1-6D, wt, and L1-KO mice revealed L1 in the immunoprecipitation from the L1-6D brain, as well as wt (but not L1-KO) mice (Fig. 1 F). The reverse immunoprecipitation of L1 from mouse brains also showed that neuropilin-1 associated with L1 from L1-6D and wt mice. Interestingly, we constantly observed that L1-6D brains contained much less L1-180 than wt brains. L1-180 is a proteolytic cleavage product of L1 in the third FNIII repeat that can be generated by plasmin (Nayeem et al., 1999) or proprotein convertase PC5A (Kalus et al., 2003). To demonstrate that sema3a signaling was preserved in L1-6D mice, we conducted growth cone collapse assays using dorsal root ganglion (DRG) neurons from P8 mouse pups and standard

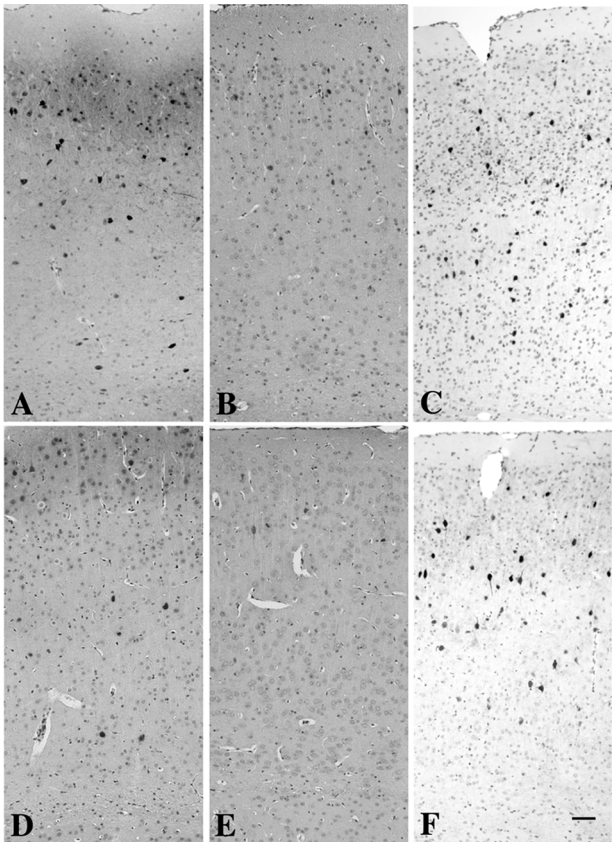

Figure 3. **GABAergic neurons of the cerebral cortex showed normal distribution in L1-6D mice.** L1-wt (A–C) and L1-6D (D–F) mice. The distribution and number of GABAergic interneurons expressing different calcium-binding proteins showed no significant differences between the two groups. A and D, calbindin; B and E, calretinin; C and F, parvalbumin, Bar, 50 μm.

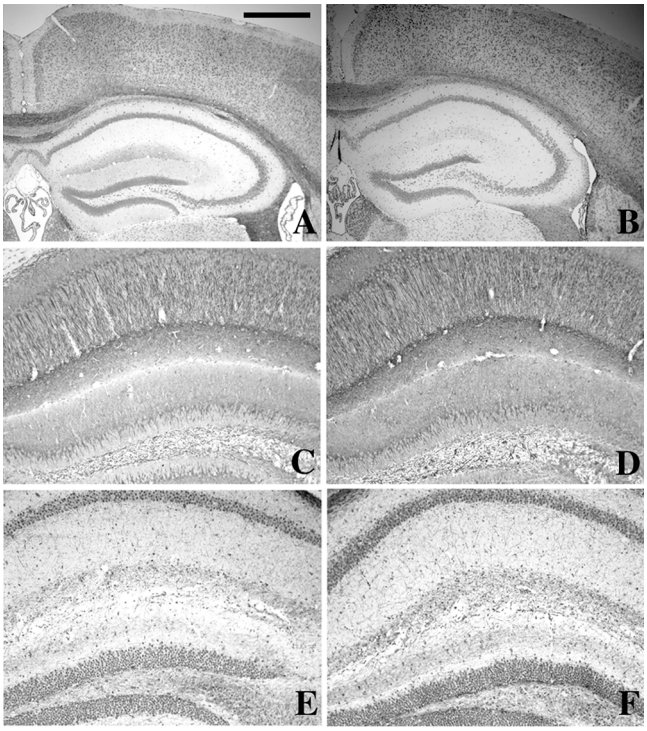

Figure 4. **Hippocampus showed normal cytoarchitecture in L1-6D mice.** L1-wt (A, C, and E) and L1-6D (B, D, and F) mice. (A and B) Cytoarchitecture of the hippocampus is normal in L1-6D mice. Kluever-Barrera stain. (C and D) Immunohistochemistry for MAP2. Dendrites of pyramidal cells in the stratum lucidum and stratum radiatum of CA regions and those of granule cells in the dentate gyrus showed no significant differences. (E and F) The distribution of neurofilament-positive neurites in the stratum lacunosum-moleculare were similar in both groups. Bar: (A and B) 500 μm; (C–F) 150 μm.

procedures. Sema3a resulted in a marked collapse of growth cones in L1-6D mice (65.7% ± 3.1; mean ± SD) and wt mice (59.3% ± 4.2), but not L1-KO mice (40.3 ± 1.5). The results from L1-6D and wt mice were not significantly different, but both were significantly different from L1-KO, at least at the 0.001 level. Untreated cultures had ∼40% collapsed growth cones. These data show that the L1–neuropilin interaction is preserved in L1-6D mice, and that this is capable of mediating growth cone collapse.

When cerebellar neurons from L1-6D mice were plated on laminin, they attached and sent out neurites in a fashion indistinguishable from control neurons (Fig. 2, A and B). In contrast, L1-6D neurons did not attach or send out neurites on L1-Fc chimeras, whereas control neurons did (Fig. 2, C and D). This is similar to the results obtained from L1-KO neurons (Fransen et al., 1998), and demonstrates that the L1-6D mice have lost L1–L1 homophilic binding. Immunohistochemical analyses of developing brain from L1-6D mice indicate that L1-6D neurons express similar amounts of L1 on their surface to control neurons (unpublished data).

Morphological analyses

The brains from L1-6D mice on the 129/Sv genetic background showed no gross anomalies with normal proportions of cerebrum, cerebellum, and brain stem, and no hydrocephalus. Histologically, the cerebrum had normal lamination with no significant neuronal loss nor decrease in white matter. The distribution and the number of GABAergic interneurons immunoreactive for different calcium-binding proteins such as parvalbumin, calbindin, and calretinin showed no significant alterations (Fig. 3). The hippocampus showed normal cytoarchitecture with no significant neuronal loss of pyramidal neurons in CA1–CA3 and of granule neurons in the dentate gyrus (Fig. 4, A and B). The direction and density of the axons and dendrites of pyramidal cells in the CA regions showed no significant differences as compared with control mice brains (Fig. 4, C–F). The mossy fibers projected normally from the granule cells in the dentate gyrus to the CA3 region. The basal ganglia showed normal cytoarchitecture, and the internal capsule was thick and well fasciculated based on neurofilament staining. The thalamus showed well-demarcated nuclei and neurofilament-immunoreactive abundant fiber bundles of thalamocortical tract. The motor nuclei, such as oculomotor nucleus, motor trigeminal nucleus, facial nucleus, and hypoglossal nucleus, substantia nigra, reticular formations, red nucleus, pontine nuclei, and inferior olivary nucleus, were observed in normal positions in the brain stem. The substantia nigra and ventral tegmental area appeared normal in the ventral tegmentum of the

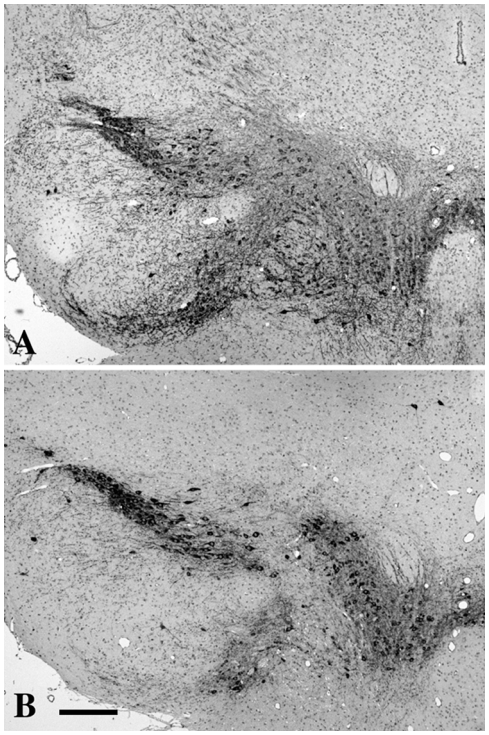

Figure 5. **Tyrosine hydroxylase–immunoreactive neurons in the midbrain of L1-6D mice had normal distributions.** L1-wt (A) and L1-6D (B) mice. The distribution of tyrosine hydroxylase–immunoreactive dopaminergic neurons showed no significant differences. Bar, 500 μm.

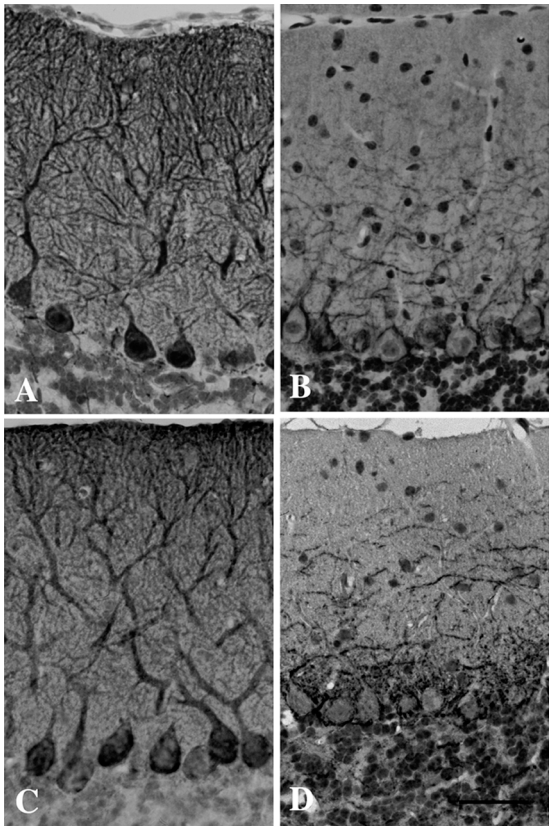

Figure 6. **The cerebellum of L1-6D mice had normal cytoarchitecture.** L1-wt (A and B) and L1-6D (C and D) mice. The dendritic tree of Purkinje cells expressing calbindin in the molecular layer (A and C); or phosphorylated neurofilament-positive axons surrounding Purkinje cells and in the molecular layer (B and D) showed no significant differences. Bar, 25 μm.

mesencephalon based on immunohistochemistry for tyrosine hydroxylase (Fig. 5, A and B).

Intensive immunohistochemical analyses showed normal appearance of calbindin-immunoreactive dendritic trees of Purkinje cells in the molecular layer, phosphorylated neurofilament-positive axons surrounding the Purkinje cells, and MAP2-immunoreactive dendrites in the molecular layer (Fig. 6, A–D).

The spinal cord showed normal cytoarchitectonic regions, laminae I–IX, and substantia gelatinosa; lamina I and II showed intense immunoreactivity for CGRP and substance P, suggesting normal nociceptive innervation of the dorsal ganglion cells in L1-6D, L1-KO, and control mice (Fig. 7, A–C). This suggests that the abnormal nociception reported in L1-KO mice (Thelin et al., 2003) is not due to abnormal projections into the spinal cord.

It has previously been shown that the corticospinal tract is abnormal in L1-KO mice (Dahme et al., 1997; Cohen et al., 1998). In contrast, in the L1-6D mice, the pyramidal tract, including subcortical white matter, internal capsule, cerebral peduncle, medullar pyramid, and dorsal column of the spinal cord, and commissural fibers such as corpus callosum, anterior, posterior, and hippocampal commissures, showed normal thickness and fiber fasciculation. The corticospinal tract was anterogradely labeled from a unilateral injection in the motor cortex. The path was observed through ipsilateral internal capsule, cerebral peduncle, pontine and medullar pyramidal tract, and pyramidal decussation at the caudal medulla and the contralateral dorsal pyramidal tract of the spinal cord as far as the Th12 level (Fig. 8, A–F). The position of the projection pathway, cross-sectional area (measured area: 3451.0 ± 769.0 in control and 3227.7 ± 640.9 as shown by pixel number), and fasciculation of the tract showed no significant differences as compared with those of control mice. In L1-KO mice, as expected, the size of pyramidal tract was significantly decreased (measured area: 1380.25 as shown by pixel number) and abnormal pyramidal decussation, showing more fibers projecting to the ipsilateral dorsal medulla, was observed. Examination of the corticothalamic and thalamocortical tracts for abnormalities in fascicle thickness or pathfinding revealed no differences between L1-6D mice and control mice (unpublished data).

When L1-KO mice are backcrossed onto the C57BL/6 genetic background, severe hydrocephalus is observed (Dahme et al., 1997). Backcrossing the L1-6D mice onto the C57BL/6 strain gave a similar dramatic result (Fig. 9). Continued backcrossing onto the C57BL/6 background produced embryonic lethality (Table I). From G5 to G9, of 157 offspring only 9 were males with the L1-6D mutation. In contrast, 63 wt males were obtained. They should be in equal proportion. In addition, the L1-6D males that were born all died before P6. Backcross of the L1-6D mutation onto the 129/Sv strain showed no evidence of embryonic lethality, whereas backcross of the L1-KO mutation gave a weak

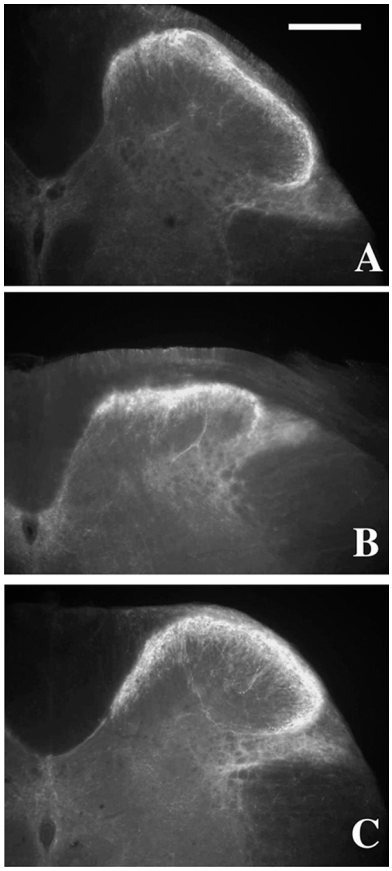

Figure 7. **Immunohistochemistry for calcitonin gene–related peptide of the cervical spinal cord.** Abundant immunoreactive fibers were observed in lamina I and II of the dorsal horn at the level of C4; a few fibers crossed at the midline, which suggested normal nociceptive innervation of DRG axons. A, L1-wt; B, L1-6D; C, L1-KO. Bar, 250 μm.

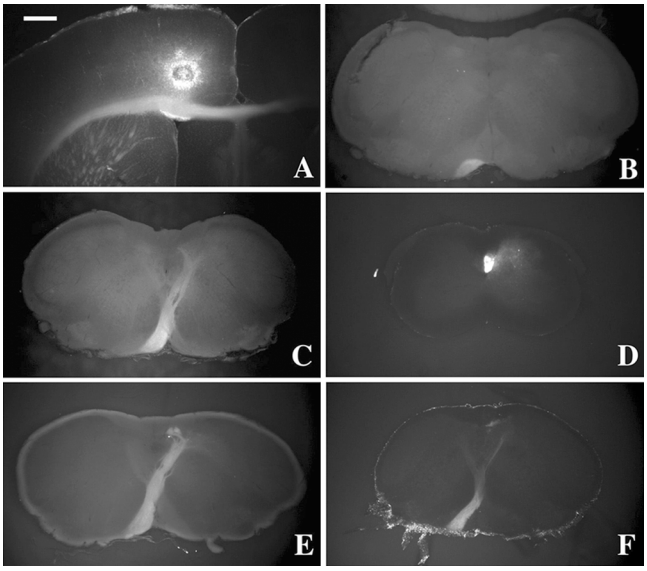

Figure 8. **Calcitonin gene–related peptide-positive DRG neurons showed normal projections into the spinal cord of L1-6D and L1-KO mice.** In L1-KO (F), the pyramidal tract was hypoplastic and labeled fibers projected to the ipsilateral dorsal medulla. A, injection site; B, pons; C, pyramidal decussation; D, spinal cord (C6) in L1-6D mouse; E, pyramidal decussation in L1-wt; F, pyramidal decussation in L1-KO mouse. Bar: (A and B) 500 μm; (C–F) 250 μm.

effect with 17% of the offspring being affected males rather than the expected 25%.

Discussion

The production of a new mouse line in which the sixth Ig domain of L1 has been deleted has provided an opportunity to study how different molecular interactions between L1 and extracellular ligands contribute to the defects observed in L1-KO mice and in humans with X-linked hydrocephalus. The L1-6D isoform of L1 is expressed on the cell surface, and based on epitope mapping, retains the expected structure of L1 minus the sixth Ig domain. The L1-6D isoform lost its ability to bind to L1 in a homophilic manner. It also lost its ability to bind α5β1 integrin. However, it retained its ability to bind to neurocan and neuropilin. L1-6D mice on the 129/Sv background are remarkably normal. Extensive examination of a variety of adult brain regions failed to reveal cytological changes, alterations in cell numbers, or changes in axon guidance. These observations are particularly important because the brain regions analyzed were selected based on their abnormal development in the L1-KO mice. However, when the L1-6D isoform was backcrossed onto C57BL/6, severe hydrocephalus developed in the offspring, and by the fifth backcross resulted in embryonic lethality for carrier males.

Since the initial publications on the phenotype of the L1-KO mice (Dahme et al., 1997; Cohen et al., 1998; Fransen et al., 1998), a number of publications have documented extensive abnormalities in these mice. Like humans with mutations in the L1 gene, L1-KO mice have a variety of defects around the midline and have alterations in neuronal morphology, axon guidance, and behavior. Thus, we were surprised to discover that many of the defects in the CNS of L1-KO mice were missing in L1-6D mice.

Recently, a transgenic mouse line with a C264Y mutation in L1 has been produced. When crossed onto the L1-KO background, a phenotype similar to L1-KO mice was obtained (Runker et al., 2003). This was not unexpected because earlier experiments had indicated that this mutation caused a disruption in cell surface expression of L1 (De Angelis et al., 2002; Michelson et al., 2002). A variety of other mutations also reduce L1 cell surface expression and, regardless of any direct affect on L1 binding, could block L1 function simply as a result of reduced expression. This explanation does not account for the changes observed in the L1-6D mice because they have normal expression patterns for L1 in the brain and on cells in the immune system.

The interaction between L1 and integrins has been intensely studied in migration of cancer cells (Montgomery et al., 1996; Duczmal et al., 1997), but only one group has examined how L1–integrin interactions participate in axon growth (Yip et al., 1998; Yip and Siu, 2001). It was reported that DRG neurons were able to send out neurites on either L1 Ig2 or L1 Ig6 domains. Neurite extension of the Ig6 domain was disrupted by mutating the RGD sites or by using anti-integrin antibodies. In contrast, retinal ganglion cells

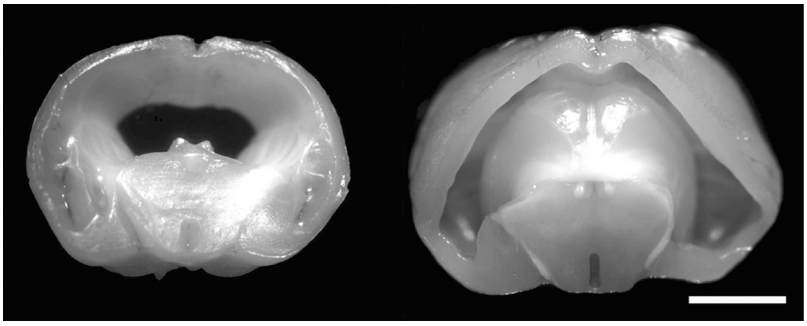

Figure 9. **Hydrocephalus in L1-6D on C57BL/6.** Crossing the L1-6D 129/Sv with C57BL/6 and then one backcross to C57BL/6 produced L1-6D males with severe hydrocephalus. Bar, 3 mm.

only sent out neurites on L1 Ig2 (Yip et al., 1998). The data argue that CNS neurons do not use integrins to bind to the RGD-containing sixth domain of L1. Our data showing that axon growth and guidance in the L1-6D mice is normal are consistent with the idea that L1–integrin interactions are not involved in axon extension in the CNS.

L1–L1 homophilic binding has been examined in a variety of systems and has been implicated in axon fasciculation, extension, and guidance (Beasley and Stallcup, 1987; Lagenaur and Lemmon, 1987; Stoeckli and Landmesser, 1995). Given the relatively high expression levels of L1 on growing axons, the dramatic effects of anti-L1 antibodies on fasciculation in a variety of in vivo and in vitro experiments, and alterations in patterns of axon growth in L1-KO mice, it is widely assumed that L1 homophilic binding is a critical component of normal CNS development. The data presented in this paper challenge this idea because L1–L1 binding has been disrupted. Previous work, especially by Kenwrick and associates (De Angelis et al., 1999, 2001, 2002), has shown that a large number of point mutations in L1 spanning the region from Ig1 to FN2 diminish or block L1–L1 homophilic binding. These same mutations also block L1–TAG-1 or L1–contactin binding, although not always to the same extent. Our data showing that neurons from L1-6D mice do not attach or send out neurites onto normal L1 are consistent with this earlier work. We failed to find decreased cross-sectional area of the corticospinal tract (Cohen et al., 1998), nor did we observe alterations in the decussation of the corticospinal tract in the medulla. We also did not see abnormalities in the corpus callosum (Demyanenko et al., 1999) or an altered distribution of dopaminergic neurons (Demyanenko et al., 2001). Because L1-KO mice on the same genetic background do have abnormalities in these projections, it is reasonable to conclude that loss of L1–L1 binding does not account for the abnormal axon growth in L1-KO mice. The same conclusion can be made regarding L1–TAG-1 and L1–contactin interactions (i.e., they do not play essential roles in the axon growth and guidance defects seen in L1-KO mice).

What might account for the axonal defects present in L1-KO mice but absent in L1-6D mice? The most likely explanation appears to be a loss of L1–neuropilin interactions in the L1-KO mice with retention of this interaction in L1-6D mice. Neuropilin is a component of the sema3a receptor. L1 has also recently been shown to be a critical component of the sema3a receptor by binding to neuropilin (Castellani et al., 2000, 2002). Neurons from L1-KO mice lose their ability to respond to sema3a. L1 and neuropilin coimmunoprecipitate, and the interaction between these two molecules has been mapped to a short peptide in the L1 first Ig domain, including the amino acids "asnkl." L1-KO mice have a defect in the pattern of decussation of the corticospinal tract in the medulla. Interestingly, sema3a expression is found at the point of corticospinal tract decussation and has been implicated in this process. Sema3a has also been shown to be involved in development of cortical apical dendrites (Polleux et al., 2000). In L1-KO mice, the dendrites of cortical neurons are abnormal (Demyanenko et al., 1999), yet we did not observe this alteration in L1-6D mice. We found that L1 and neuropilin coimmunoprecipitate in L1-6D mice and that sema3a was capable of inducing growth cone collapse in DRG neurons from L1-6D mice but not in L1-KO mice. The presence of defects in axon and dendrite growth in the L1-KO mice that can be attributed to a loss of sema3a signaling and the absence of those defects in the L1-6D mice makes a strong case that the L1–neuropilin interaction that participates in sema3a signaling is a critical factor in the major CNS defects observed in L1-KO mice and in some humans with X-linked hydrocephalus.

Table I. **Viability on different genetic backgrounds**

	L1-KO					L1-6D				
	m −/Y	**m +/Y**	**f −/+**	**f +/+**	**# of mice**	**m −/Y**	**m +/Y**	**f −/+**	**f +/+**	**# of mice**
	%	%	%	%		%	%	%	%	
Expected	25	25	25	25	-	25	25	25	25	-
129/Sv	17	36	20	27	222	25	22	24	29	130
C57BL/6	5	38	23	34	229	6	40	17	37	157

On the 129/Sv genetic background, both L1-KO and L1-6D produced a slightly lower percentage of mutant males than expected. However, on the C57BL/6 genetic background, after five generations of backcross there was a severe lethality with only a small percentage of affected males being born for either L1-KO or L1-6D. Of the −/Y males that were born, none survived until P6. These data are from a compilation of births from G5 to G9.

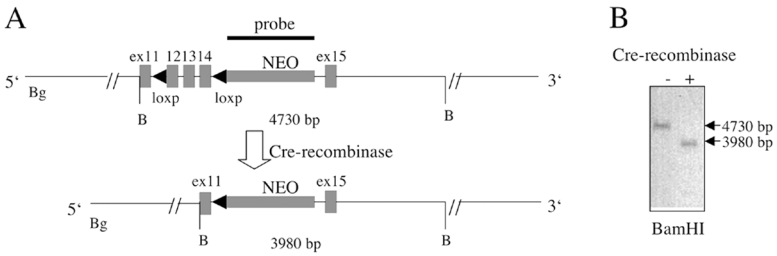

Figure 10. **Targeting strategy for production of L1-6D mice.** (A) Restriction map of part of the L1 gene using BamH1, insertion sites of loxP sites (black triangle), and neomycin cassette and expected structure after crossing to Cre-recombinase containing mice. (B) Southern blot analysis of DNA from L1-6D mice before and after cross with Cre-recombinase mice showing expected size of fragments after BamH1 digestion.

When L1-6D mice were backcrossed onto the C57BL/6 background, severe hydrocephalus occurred and by the fifth backcross the L1-6D mutation was an embryonic lethal in the vast majority of cases. The severe consequences of the L1-6D mutation of the C57BL/6 background are consistent with earlier experiments on L1-KO mice (Dahme et al., 1997). They are also reminiscent of human mutations that cause X-linked hydrocephalus. There are numerous examples of families where one affected individual has severe hydrocephalus and a sibling with the same mutation has relatively mild CNS abnormalities. Our data are consistent with the hypothesis that a loss of L1 homophilic binding on the C57BL/6 background is sufficient to cause hydrocephalus. Because TAG-1 KO mice (Fukamauchi et al., 2001), F3/contactin KO mice (Berglund et al., 1999), and β1 integrin mice (Graus-Porta et al., 2001) do not show hydrocephalus, it seems unlikely that the cause of hydrocephalus on the C57BL/6 background is loss of L1 interactions with any of these proteins. The simplest explanation is that the loss of L1–L1 homophilic binding is important in the generation of hydrocephalus, but it is not possible to know for sure based on our data. Determining if L1 homophilic binding or heterophilic binding to TAG-1, F3, or β1 integrins mediates hydrocephalus may be difficult because in vitro analyses show that most point mutations that alter L1–L1 binding also alter L1–F3 and L1–TAG-1 binding. The fact that L1-NrCAM double KOs are embryonic lethal on the 129/Sv background (Sakurai et al., 2001), along with earlier data on L1-KO mice and our present data, supports the hypothesis that the C57BL/6 background has a gene(s) that interacts with L1 to cause the severe CNS abnormalities. Identification of this gene(s) may be challenging because recovery of all affected offspring in backcross experiments is difficult.

The results from this work also have implications for the hypothesis that fetal alcohol syndrome (FAS) is due, in part, to disruption of L1–L1 binding (Ramanathan et al., 1996). It was noted that patients with FAS have some common features with individuals with X-linked hydrocephalus. Subsequently, it was reported that alcohols can disrupt L1-mediated adhesion, but this result has been challenged (Vallejo et al., 1997; Bearer et al., 1999). It has also been reported that alcohol can inhibit L1-mediated axon growth (Bearer et al., 1999). The fact that L1-6D mice do not have axon growth or guidance defects in the 129/Sv background argues strongly that a loss of L1–L1 adhesion does not underlie the abnormalities in FAS.

In conclusion, L1-6D mice brains showed normally developed axon pathways as well as appropriate anatomical features on the 129/Sv background. These results show that axonal guidance and neuronal migration can proceed without L1–L1 homophilic binding. The embryonic lethality on the C57BL/6 background shows that in some genetic backgrounds, L1-mediated adhesion is essential for CNS development. Finally, our data raise the possibility that many of the CNS defects observed in L1-KO mice are due to a loss of sema3a signaling mediated by L1–neuropilin interactions.

Materials and methods

Animals

All animal experiments described in this manuscript have been approved by our institutional review boards. The mouse in which the sixth Ig domain of L1 was deleted (L1-6D) was generated using a cre/lox approach (Fig. 10). In brief, in embryonic stem cells, loxP sites were inserted in the L1 gene via homologous recombination into introns 11 and 14. The embryonic stem cells were injected into blastocysts, and these were transferred into mice. Mice carrying the lox sites were crossed multiple times to obtain mice homozygous for the inserts (L1-6DloxP). These mice were then crossed to Cre-expressing mice to produce a specific KO of the sixth Ig domain. These mice are missing exons 12, 13, and 14 and have a neo cassette immediately preceding exon 15. Lymphocytes from the L1-6D mice were analyzed for L1 expression using FACS® analysis and showed a loss of the expression of the sixth Ig domain epitope, but retain the other important regions of the L1 gene product. For control mice, we used the mice carrying the targeting loxP site but expressing the sixth domain of L1.

Genetic backcrosses

Mice with loxP sites surrounding the L1-6D exons (L1-6DloxP) or deleted L1-6D exons (L1-6D) were backcrossed onto 129/Sv or C57BL/6 background for 5–10 generations. Genotyping was done using PCR methods. Primers for detecting L1-6D mutants: forward, 5′-CCAGCCAGGATCCTAACAAAAGAC-3′; reverse, 5′-GCAGGGCTCCAAGACAAGTGC-3′. Primers for detecting L1-6DloxP mice: forward, 5′-CCAGCCAGGATCCTAACAAAAGAC-3′; reverse, 5′-GTGGAGAGGCTATTCGGCTATGA-3′.

Fluorescent staining

The staining of cells with mAbs and FITC-conjugated goat antibodies to rat Ig has been described previously (Mechtersheimer et al., 2001). Stained cells were analyzed with a FACScan™ analyzer (Becton Dickinson).

Affinity purification of L1

L1 immunoaffinity purification was done essentially as described before (Ruppert et al., 1995). In brief, a 1% Triton X-100 lysate was prepared from brain and spleen and passed over a nonspecific rat IgG-Sepharose column followed by an mAb 555 Sepharose column. The column was washed extensively and then eluted with 100 mM diethylamine/HCl, pH 11.5, and 150 mM NaCl containing 50 mM β-octyl-glucopyranoside. Fractions of the eluate were neutralized and analyzed by ELISA.

Biochemical analysis

Cell lysate was mixed with SDS sample buffer and proteins were separated by SDS-PAGE under reducing conditions. After transfer to an Immobilon membrane by semi-dry blotting, membranes were blocked with 5% skim milk in TBS. Blots were developed with mAbs specific for L1 followed by peroxidase-conjugated goat anti–rat IgG and ECL detection (Amersham Biosciences).

Analysis of neurocan binding by dot blot immunoassay

For the analysis of L1–neurocan interaction, 0.5 μg neurocan was adsorbed to Immobilon membranes (Millipore) using a dot blot apparatus as

described previously (Oleszewski et al., 2000). Membranes were incubated with 100 μg/ml purified L1 protein, and bound L1 was detected by mAb 555 followed by the respective secondary antibodies and ECL detection as described above for Western blots.

Analysis of L1–neuropilin interactions

To examine L1–neuropilin interactions, brains were lysed in 1 ml immunoprecipitation buffer (25 mM Hepes, 5 mM EDTA, 1 mM $MgCl_2$, 2 mM PMSF, 10% glycerol, and 1% Triton X-100; Castellani et al., 2000). Lysates were incubated at 4°C for 30 min, centrifuged for 15 min, and precleared with protein A–Sepharose for 2 h at 4°C. Samples were immunoprecipitated with 1 μg 555 (L1) or with 1 μg anti-NRPI (Oncogene Research Products) overnight at 4°C followed by incubation with Protein G for 1 h at 4°C. This was followed by Western blotting with anti-L1 (555) and anti-neuropilin antibodies.

Collapse assay

The sema3a expression plasmid Coll-pAG-NT was a gift from J. Raper (Koppel and Raper, 1998). COS-7 cells were grown in DME with 10% FBS and 2 mM GlutaMAX™ and were transfected using the Nucleofector™ kit (Amaxa) according to the manufacturer's protocol. Conditioned medium was collected 2 d after transfection and spun down to remove debris. Supernatants were stored in frozen aliquots before their use in the growth cone collapse assay. Western blot with anti-myc antibody was performed to verify the presence of sema3a in the supernatants. DRGs from P8 mice were dissected and dissociated into single cells with dispase and deoxynuclease treatment. Dissociated DRG cells were plated onto LabTek™ 4-well chambered slides (Nunc) coated with poly-lysine and laminin. The procedure for the collapse assay was essentially the same as described previously (Raper and Kapfhammer, 1990). In brief, 200-μl aliquots of sema3a supernatants were added to 500 μl culture medium and mixed well. The cultures were incubated at 37°C in 5% CO_2 for 1 h. Cultures were then fixed with 4% PFA in PBS. Growth cones without lamellipodia or filopodia were scored as collapsed.

Cell adhesion assays

Binding of B16F10 melanoma cells to purified L1 or FN was done as described previously (Ruppert et al., 1995; Oleszewski et al., 2000). In brief, L1 in β-octyl-glucopyranoside (~100 μg/ml) was diluted 1:10 with TBS and coated to LabTek™ glass chamber slides (Nunc). FN was coated at 10 μg/ml. Wells were then blocked with 1% ovalbumin in TBS and washed with HBSS containing 10 mM Hepes, 2 mM Ca^{2+}, and 2 mM Mg^{2+} (binding buffer). B16F10 cells (5–10 × 10^6/ml) in binding buffer were added to the coated slides. The binding assay was performed for 30 min at RT without shaking, and the slides were fixed in 2% glutaraldehyde/PBS after briefly dipping into PBS. Bound cells were counted by video microscopy using Image 1.52 software (National Institutes of Health, Bethesda, MD). Data are presented as mean values plus SEM.

Cerebellar granule cells from P8 L1-6D or control 129/Sv mice were dissociated using trypsin and were plated on dishes coated with laminin or L1-Fc as described previously (Fransen et al., 1998). After 18 h, the dishes were examined for attachment and neurite growth.

Histology and immunohistochemistry

For the morphological analysis, adult mice (8 wk of age) were anesthetized by an i.p. injection of a mixture of ketamine, xylazine, and acepromazine, and perfused transcardially with 4% PFA in 0.1 M sodium phosphate buffer, pH 7.3. Brains and spinal cord were removed and post-fixed at 4°C overnight in the same fixative and embedded in paraffin. Embryos (E17) were extracted from the uterus and immediately immersed in the same fixatives at 4°C overnight. 5-μm-thick sections were cut coronally or sagitally for immunohistochemistry, and serial 15-μm-thick sections were cut for Kluever-Barrera stain. Immunohistochemistry for each antigen was performed on 5-μm-thick paraffin sections, following standard protocols for the PAP method. After deparaffinization and quenching of endogenous peroxidase activity by immersing the sections in 3% hydrogen peroxide in methanol for 30 min, antigen retrieval using microwave heating was performed for immunohistochemistry against anti-neurofilament, anti-MAP2, and anti-calbindin-D-28K. Sections were placed into 10 mM citrate buffer (pH 7.0), then microwaved at 750 W for a total of 9–21 min, with brief interruptions every 3 min to replace the evaporated volume with distilled water. The slides were then cooled to RT in the citrate buffer and transferred to PBS. The sections were blocked in 10% normal goat serum and 1% BSA in PBS, and were then incubated with primary antibodies at 4°C overnight. Sections were rinsed in PBS and incubated in secondary antibodies conjugated with HRP-labeled polymer (EnVision™; DakoCytomation) according to the manufacturer's protocol. The reaction product was visualized with DAB. As controls, the primary antiserum was replaced by normal serum at appropriate dilution. Primary antibodies were used for immunostaining as follows: anti-neurofilament (RT97, 1:1,000), anti-MAP2 (1:1,000; Sigma-Aldrich), anti-tau-1 (1:1,000; CHEMICON International), anti-calbindin-D-28K (1:2,000; Sigma-Aldrich), anti-parvalbumin (1:2,000; CHEMICON International), anti-calretinin (1:500; CHEMICON International), anti-tyrosine hydroxylase (1:500; CHEMICON International), and anti-L1CD (1:1,000; V. Lemmon). The cerebrum, hippocampus, thalamus, basal ganglia, brain stem, cerebellum, and spinal cord were examined.

DiI labeling of the corticospinal and thalamocortical tracts in adult mice

For 1,1′-dioctadecyl-3,3,3′,3′-tetramethylindocarbocyaminide perchloride (DiI; Molecular Probes, Inc.) labeling of the corticospinal tract, adult mice (8 wk of age) were anesthetized by an i.p. injection of a mixture of ketamine, xylazine, and acepromazine. After skin incision of the scalp, a small burr hole was made in the skull at 0.5 mm rostral to bregma using a dental drill. Small crystals of DiI were inserted into the motor cortex. After the injection, the scalp was sutured, bupivacaine was applied to the suture site, and the animals were allowed to recover from anesthesia. After 8–10 wk of post-injection survival time, the animals were perfused transcardially with 4% PFA in 0.1 M sodium phosphate buffer, pH 7.3. Brains and spinal cord were removed and post-fixed at 4°C overnight in the same fixative. 70–100-μm-thick coronal and sagittal vibratome sections were cut and analyzed by fluorescence microscopy. Small crystals of DiI were inserted into the occipital cortex for corticothalamic tract labeling and into the dorsal thalamic nuclei for thalamocortical tract analyses using fixed brains, and were incubated in 4% PFA at 37°C for 2–4 wk. Vibratome sections of the brains were cut coronally or sagitally at 100-μm thicknesses. Photomicroscopy was done on a microscope (model DMLB; Leica), and images were acquired with a camera (RT Slider Spot; Diagnostic Instruments). Adobe Photoshop® 7.0 was used to prepare the images for publication.

The authors are grateful for the technical assistance of Eli Weaver, Maryanne Pendergast, and Denice Major, and for discussions with Karl Herrup and Ron Conlon. We also thank J. Raper for supplying the sema3a expression vector. The contributions of Matthias Oleszewski in the initial phase of the project and the technical help from Günther Kübelbeck are gratefully acknowledged.

V. Lemmon was supported by grants from the National Institutes of Health (CHD-HD39884, EY-05285, and EY-11373) and RIKEN. B. Arnold was supported by a grant from Sonderforschungsbereich 405, and P. Altevogt by a grant from Scheel Stiftung (Bonn, Germany). V. Lemmon holds the Walter G. Ross Chair in Developmental Neuroscience at the University of Miami.

Submitted: 16 December 2003
Accepted: 25 February 2004

References

Bearer, C.F., A.R. Swick, M.A. O'Riordan, and G. Cheng. 1999. Ethanol inhibits L1-mediated neurite outgrowth in postnatal rat cerebellar granule cells. *J. Biol. Chem.* 274:13264–13270.

Beasley, L., and W.B. Stallcup. 1987. The nerve growth factor-inducible large external (NILE) glycoprotein and neural cell adhesion molecule (N-CAM) have distinct patterns of expression in the developing rat central nervous system. *J. Neurosci.* 7:708–715.

Berglund, E.O., K.K. Murai, B. Fredette, G. Sekerkova, B. Marturano, L. Weber, E. Mugnaini, and B. Ranscht. 1999. Ataxia and abnormal cerebellar microorganization in mice with ablated contactin gene expression. *Neuron.* 24: 739–750.

Castellani, V., A. Chedotal, M. Schachner, C. Faivre-Sarrailh, and G. Rougon. 2000. Analysis of the L1-deficient mouse phenotype reveals cross-talk between Sema3A and L1 signaling pathways in axonal guidance. *Neuron.* 27: 237–249.

Castellani, V., E. De Angelis, S. Kenwrick, and G. Rougon. 2002. Cis and trans interactions of L1 with neuropilin-1 control axonal responses to semaphorin 3A. *EMBO J.* 21:6348–6357.

Cohen, N.R., J.S. Taylor, L.B. Scott, R.W. Guillery, P. Soriano, and A.J. Furley. 1998. Errors in corticospinal axon guidance in mice lacking the neural cell adhesion molecule L1. *Curr. Biol.* 8:26–33.

Dahme, M., U. Bartsch, R. Martini, B. Anliker, M. Schachner, and N. Mantei. 1997. Disruption of the mouse L1 gene leads to malformations of the nervous system. *Nat. Genet.* 17:346–349.

De Angelis, E., J. MacFarlane, J.S. Du, G. Yeo, R. Hicks, F.G. Rathjen, S. Kenwrick, and T. Brummendorf. 1999. Pathological missense mutations of neural cell adhesion molecule L1 affect homophilic and heterophilic binding activities. *EMBO J.* 18:4744–4753.

De Angelis, E., T. Brummendorf, L. Cheng, V. Lemmon, and S. Kenwrick. 2001. Alternative use of a mini exon of the L1 gene affects L1 binding to neural ligands. *J. Biol. Chem.* 276:32738–32742.

De Angelis, E., A. Watkins, M. Schafer, T. Brummendorf, and S. Kenwrick. 2002. Disease-associated mutations in L1 CAM interfere with ligand interactions and cell-surface expression. *Hum. Mol. Genet.* 11:1–12.

Demyanenko, G.P., A.Y. Tsai, and P.F. Maness. 1999. Abnormalities in neuronal process extension, hippocampal development, and the ventricular system of L1 knockout mice. *J. Neurosci.* 19:4907–4920.

Demyanenko, G.P., Y. Shibata, and P.F. Maness. 2001. Altered distribution of dopaminergic neurons in the brain of L1 null mice. *Brain Res. Dev. Brain Res.* 126:21–30.

Duczmal, A., S. Schollhammer, S. Katich, O. Ebeling, R. Schwartz-Albiez, and P. Altevogt. 1997. The L1 adhesion molecule supports αvβ3-mediated migration of human tumor cells and activated T lymphocytes. *Biochem. Biophys. Res. Commun.* 232:236–239.

Fransen, E., R. D'Hooge, G. Van Camp, M. Verhoye, J. Sijbers, E. Reyniers, P. Soriano, H. Kamiguchi, R. Willemsen, S.K. Koekkoek, et al. 1998. L1 knockout mice show dilated ventricles, vermis hypoplasia and impaired exploration patterns. *Hum. Mol. Genet.* 7:999–1009.

Fukamauchi, F., O. Aihara, Y.J. Wang, K. Akasaka, Y. Takeda, M. Horie, H. Kawano, K. Sudo, M. Asano, K. Watanabe, and Y. Iwakura. 2001. TAG-1-deficient mice have marked elevation of adenosine A1 receptors in the hippocampus. *Biochem. Biophys. Res. Commun.* 281:220–226.

Graus-Porta, D., S. Blaess, M. Senften, A. Littlewood-Evans, C. Damsky, Z. Huang, P. Orban, R. Klein, J.C. Schittny, and U. Muller. 2001. β1-class integrins regulate the development of laminae and folia in the cerebral and cerebellar cortex. *Neuron.* 31:367–379.

Jacob, J., J. Haspel, N. Kane-Goldsmith, and M. Grumet. 2002. L1 mediated homophilic binding and neurite outgrowth are modulated by alternative splicing of exon 2. *J. Neurobiol.* 51:177–189.

Kalus, I., B. Schnegelsberg, N.G. Seidah, R. Kleene, and M. Schachner. 2003. The proprotein convertase PC5A and a metalloprotease are involved in the proteolytic processing of the neural adhesion molecule L1. *J. Biol. Chem.* 278: 10381–10388.

Kamiguchi, H., M.L. Hlavin, M. Yamasaki, and V. Lemmon. 1998. Adhesion molecules and inherited diseases of the human nervous system. *Annu. Rev. Neurosci.* 21:97–125.

Kenwrick, S., A. Watkins, and E. De Angelis. 2000. Neural cell recognition molecule L1: relating biological complexity to human disease mutations. *Hum. Mol. Genet.* 9:879–886.

Koppel, A.M., and J.A. Raper. 1998. Collapsin-1 covalently dimerizes, and dimerization is necessary for collapsing activity. *J. Biol. Chem.* 273:15708–15713.

Lagenaur, C., and V. Lemmon. 1987. An L1-like molecule, the 8D9 antigen, is a potent substrate for neurite extension. *Proc. Natl. Acad. Sci. USA.* 84:7753–7757.

Mechtersheimer, S., P. Gutwein, N. Agmon-Levin, A. Stoeck, M. Oleszewski, S. Riedle, R. Postina, F. Fahrenholz, M. Fogel, V. Lemmon, and P. Altevogt. 2001. Ectodomain shedding of L1 adhesion molecule promotes cell migration by autocrine binding to integrins. *J. Cell Biol.* 155:661–673.

Michelson, P., C. Hartwig, M. Schachner, A. Gal, A. Veske, and U. Finckh. 2002. Missense mutations in the extracellular domain of the human neural cell adhesion molecule L1 reduce neurite outgrowth of murine cerebellar neurons. *Hum. Mutat.* 20:481–482.

Montgomery, A.M., J.C. Becker, C.H. Siu, V.P. Lemmon, D.A. Cheresh, J.D. Pancook, X. Zhao, and R.A. Reisfeld. 1996. Human neural cell adhesion molecule L1 and rat homologue NILE are ligands for integrin αvβ3. *J. Cell Biol.* 132:475–485.

Nayeem, N., S. Silletti, X. Yang, V.P. Lemmon, R.A. Reisfeld, W.B. Stallcup, and A.M. Montgomery. 1999. A potential role for the plasmin(ogen) system in the posttranslational cleavage of the neural cell adhesion molecule L1. *J. Cell Sci.* 112:4739–4749.

Oleszewski, M., P. Gutwein, W. von der Lieth, U. Rauch, and P. Altevogt. 2000. Characterization of the L1-neurocan-binding site. Implications for L1-L1 homophilic binding. *J. Biol. Chem.* 275:34478–34485.

Polleux, F., T. Morrow, and A. Ghosh. 2000. Semaphorin 3A is a chemoattractant for cortical apical dendrites. *Nature.* 404:567–573.

Ramanathan, R., M.F. Wilkemeyer, B. Mittal, G. Perides, and M.E. Charness. 1996. Alcohol inhibits cell-cell adhesion mediated by human L1. *J. Cell Biol.* 133:381–390.

Raper, J.A., and J.P. Kapfhammer. 1990. The enrichment of a neuronal growth cone collapsing activity from embryonic chick brain. *Neuron.* 4:21–29.

Runker, A.E., U. Bartsch, K.A. Nave, and M. Schachner. 2003. The C264Y missense mutation in the extracellular domain of L1 impairs protein trafficking in vitro and in vivo. *J. Neurosci.* 23:277–286.

Ruppert, M., S. Aigner, M. Hubbe, H. Yagita, and P. Altevogt. 1995. The L1 adhesion molecule is a cellular ligand for VLA-5. *J. Cell Biol.* 131:1881–1891.

Sakurai, T., M. Lustig, J. Babiarz, A.J. Furley, S. Tait, P.J. Brophy, S.A. Brown, L.Y. Brown, C.A. Mason, and M. Grumet. 2001. Overlapping functions of the cell adhesion molecules Nr-CAM and L1 in cerebellar granule cell development. *J. Cell Biol.* 154:1259–1273.

Schaefer, A.W., Y. Kamei, H. Kamiguchi, E.V. Wong, I. Rapoport, T. Kirchhausen, C.M. Beach, G. Landreth, S.K. Lemmon, and V. Lemmon. 2002. L1 endocytosis is controlled by a phosphorylation-dephosphorylation cycle stimulated by outside-in signaling by L1. *J. Cell Biol.* 157:1223–1232.

Silletti, S., F. Mei, D. Sheppard, and A.M. Montgomery. 2000. Plasmin-sensitive dibasic sequences in the third fibronectin-like domain of L1-cell adhesion molecule (CAM) facilitate homomultimerization and concomitant integrin recruitment. *J. Cell Biol.* 149:1485–1502.

Stoeckli, E.T., and L.T. Landmesser. 1995. Axonin-1, Nr-CAM, and Ng-CAM play different roles in the in vivo guidance of chick commissural neurons. *Neuron.* 14:1165–1179.

Thelin, J., A. Waldenstrom, U. Bartsch, M. Schachner, and J. Schouenborg. 2003. Heat nociception is severely reduced in a mutant mouse deficient for the L1 adhesion molecule. *Brain Res.* 965:75–82.

Vallejo, Y., M. Hortsch, and R.R. Dubreuil. 1997. Ethanol does not inhibit the adhesive activity of *Drosophila* neuroglian or human L1 in *Drosophila* S2 tissue culture cells. *J. Biol. Chem.* 272:12244–12247.

Weller, S., and J. Gartner. 2001. Genetic and clinical aspects of X-linked hydrocephalus (L1 disease): Mutations in the L1CAM gene. *Hum. Mutat.* 18:1–12.

Yamasaki, M., P. Thompson, and V. Lemmon. 1997. CRASH syndrome: mutations in L1CAM correlate with severity of the disease. *Neuropediatrics.* 28: 175–178.

Yip, P.M., and C.H. Siu. 2001. PC12 cells utilize the homophilic binding site of L1 for cell-cell adhesion but L1-αvβ3 interaction for neurite outgrowth. *J. Neurochem.* 76:1552–1564.

Yip, P.M., X. Zhao, A.M. Montgomery, and C.H. Siu. 1998. The Arg-Gly-Asp motif in the cell adhesion molecule L1 promotes neurite outgrowth via interaction with the αvβ3 integrin. *Mol. Biol. Cell.* 9:277–290.

Zhao, X., and C.H. Siu. 1995. Colocalization of the homophilic binding site and the neuritogenic activity of the cell adhesion molecule L1 to its second Ig-like domain. *J. Biol. Chem.* 270:29413–29421.

Zhao, X., P.M. Yip, and C.H. Siu. 1998. Identification of a homophilic binding site in immunoglobulin-like domain 2 of the cell adhesion molecule L1. *J. Neurochem.* 71:960–971.